

# Orbit Determination of Meteors Using the MU Radar

Toru SATO<sup>†</sup>, Takuji NAKAMURA<sup>††</sup>, *Members*, and Koji NISHIMURA<sup>†</sup>, *Nonmember*

**SUMMARY** Meteor storms and showers are now considered as potential hazard in the space environment. Radar observations of meteors has an advantage of a much higher sensitivity over optical observations. The MU radar of Kyoto University, Japan has a unique capability of very fast beam steerability as well as a high sensitivity to the echoes from ionization around the meteors. We developed a special observation scheme which enables us to determine the orbit of individual meteors. The direction of the target is determined by comparing the echo intensity at three adjacent beams. The Doppler pulse compression technique is applied to improve the signal-to-noise ratio of the echoes from the very fast target, and also to determine the range accurately. The developed scheme was applied to the observation made during the Leonid meteor storm on November 18, 1998 (JST). Estimated orbital distribution seems to suggest that the very weak meteors detected by the MU radar are dominated by sporadic meteors rather than the stream meteors associated with the Leonids storm.

*key words:* meteor observation, MU radar, orbit determination, Doppler pulse compression, space environment

## 1. Introduction

Space debris has widely been recognized as a potential hazard for the space environment. While collisions with relatively large artificial objects of larger than 1 cm size will cause a catastrophic damage for rare occasions, more frequent collisions with much smaller natural meteoroids usually cause minor damages to the surface of satellites. Among meteoroids, distinct meteor storms and showers are the most threatening natural events in the space.

A substantial maximum of the Leonid meteors was observed worldwide around November 18, 1998, and also in 1999. The very large impinging velocity of 72 km/s, which is close to the maximum relative velocity of two bodies encountering in the solar system, will largely enhance the damage in the event of collision. In order to make a precise prediction of the possible damage due to this meteor shower, it is important to study the statistics of the orbit of meteors. Optical observations of Leonids provided very accurate orbit of the stream meteors[1], but they are limited to large objects which has a very low probability of collision with satellites. Radar observations of meteors has an advantage of a much higher sensitivity over optical observations, providing valuable information on the meteors of very small sizes whose collision probability cannot be neglected. However, the or-

bit determination has been a difficult task because it requires flexible antenna beam configuration as well as a very high sensitivity.

We have developed a special observation scheme of this event for the MU (Middle and Upper atmosphere) radar of Japan, which is a powerful VHF Doppler radar equipped with an active phased array antenna of 100 m size. The technique is basically the same as that used to monitor space debris, but modified to detect meteors with much higher velocity. The major improvement is the implementation of the Doppler pulse compression scheme as described in Section 4, which enables us to detect very fast meteors with high sensitivity.

Here we describe the technique and some preliminary results obtained during the observation made on November 18, 1998.

## 2. MU radar observation of space debris and meteors

Radar observation is the most practical way of studying the space debris environment on the low-earth orbit as far as the objects of larger than 1 cm are concerned[2].

The MU radar of Japan is originally designed to observe backscattering from turbulent fluctuations in the refractive index of the atmosphere[3], and thus has the lowest frequency (46.5 MHz) among all radars used for debris observation. Since the radar backscattering cross-section (RCS) is proportional to the 6th power of size for objects smaller than the radar wavelength, it is disadvantageous to employ a wavelength of as long as 6.4 m in detecting small objects. However, the reduced RCS of small debris is compensated for by the large antenna aperture and the high output power, so that the radar has shown comparable sensitivity in space debris detection to those employed by US SPACECOM for routine monitoring of space debris[4].

In observations of meteors, on the other hand, a lower frequency has the advantage of higher sensitivity because the echo is due to scattering and reflection from the ionized plasma created around the meteors collisions with the surrounding atmospheric molecules at the height of about 100 km. When a meteor impinges the atmosphere, a column of such ionization remains after the trace of the meteor, usually for a fraction of a second. Meteor radar is a type of radar designed to detect strong specular reflection from such ionized trails produced when the line-of-sight direction is perpendicular to the trail[5]. It is also possible to observe

Manuscript received December 21, 1999.

Manuscript revised March 25, 2000.

<sup>†</sup>The authors are with Department of Communication and Computer Engineering, Graduate School of Informatics, Kyoto University, Kyoto 606-8501, Japan.

<sup>††</sup>The author is with Radio Science Center for Space and Atmosphere, Kyoto University, Uji 611-0011, Japan.

the scattering from the plasma around the meteor itself if the sensitivity of the radar is sufficiently high[6], as is the case for the MU radar. This type of echoes are called meteor head echoes in contrast to the trail echoes. While the analysis of trail echoes provide the information mainly on the atmosphere, those of head echoes give more direct information on the meteor itself[7]. However, previous observations of meteor head echoes were limited to statistics of detection frequency and impinging velocity, because the high power atmospheric radars as used in [6] do not have tracking capability against moving targets, with the MU radar being the only exception. Here we make the best use of the fast beam steerability of the MU radar in determining the orbit of individual meteors.

### 3. Determination of directions

The antenna beam of the MU radar has a one-way half-power width of  $3.7^\circ$ , and can be pointed to any desired direction within a coverage of  $30^\circ$  from the zenith in a switching time of  $10 \mu\text{s}$ . It is therefore possible to observe the passage of an object with multiple beams. We developed a special debris observation mode with which the antenna beam is switched alternately from pulse to pulse among 8 directions arranged closely around the zenith[8]. Although the antenna pattern deforms as the pointing direction deviates from the zenith, the effect is inversely proportional to cosine of the zenith angle, and is readily accounted for in the computation.

Accurate instantaneous direction of the object is determined by comparing the echo intensity from consecutive pulses with different beam directions assuming that the scattering cross section does not vary for the two pulses, and that the antenna pattern is precisely known. Validity of the former assumption is examined in some details later, while the latter assumption has been confirmed by the antenna pattern measurement using the moon reflection method[9].

During the observation of Leonid meteors, the antenna beam was switched alternately among 7 directions with a cycle of 8 pulses at the inter-pulse period of 5.12 ms around the expected radiant of the Leonid meteors. Six 15-min observations were made during the 6-hour period while the elevation of the radiant is above  $60^\circ$ . The left panel of Fig. 1 shows a plan view of the 8 beams. The abscissa and the ordinate is the east-west and the north-south angles, respectively, as measured from the center of the beam groups. Center of the beams are arranged to constitute 6 equilateral triangles at  $3^\circ$  intervals. Note that beam No. 1 and 5 observe the same direction. The sequence of the beams are chosen so that every set of 3 consecutive pulses constitute an equilateral triangle. By this arrangement, the location of the target can be determined within two inter-pulse period of 10.24 ms. While it is possible to cover wider angular region by increasing the number of beams, the sampling interval between two beam cycles becomes prohibitively long to track the meteors.

If a target is located within  $3^\circ$  from the center of the center beam, the ratio of the echo power between the two adjacent beams falls within the range of  $\pm 18 \text{ dB}$ , whose value

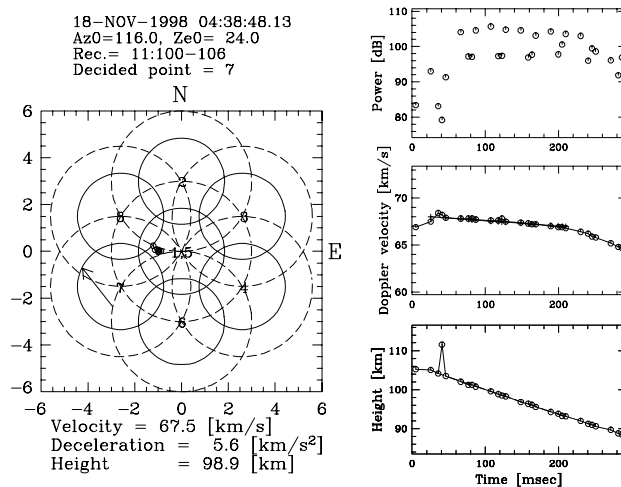


**Fig. 1** Example of orbit determination. Angular position (left) and the variation of echo power (top right), Doppler velocity (middle right), and height (bottom right) versus time after detection.

gives the relative location of the target between the beam centers. A smaller angular separation than  $3^\circ$  gives a smaller dynamic range of echoes, which enables us to make use of weaker echoes, but at the cost of reduced angular coverage. A careful study is needed to determine the optimum separation between the beams.

The accuracy of determined direction is estimated to be about  $0.13^\circ$  for the case of satellites with sufficiently large cross section[8]. Instantaneous direction of a meteor thus determined from 3 adjacent pulses are plotted by small circle symbols on the left panel of the figure. The arrow indicates the direction of the mean progression of these points on the angular plane. Solid and dashed circles roughly indicate the coverage of each beam, which is  $3^\circ$  and  $6^\circ$ , respectively.

Besides the assumptions stated above, this method of angular determination also postulates that the observed echoes are coming from the main lobe region of the antenna. Considering the very high sensitivity of the radar, it should be examined whether the magnitude of the meteor head echoes is strong enough to be observed through the sidelobes. In order to examine this possibility in a statistical manner, a simple simulation is made. Circles and the solid line in Fig. 2 shows the number distribution of observed echoes versus their signal-to-noise ratio in a log-log scale. If these echoes are mainly observed from the main lobe region, which covers a  $6^\circ$  cone in the sky, we can estimate the number of meteors with similar magnitude over the entire sky, which is about 33 dB larger in the solid angle than the main lobe region. Since the average sidelobe level in the two-way pattern is known to be about 50 dB lower than the main lobe level, we can thus estimate the number distribution of echoes in the sidelobe region by shifting the solid line 50 dB to the left and 33 dB to the top. Triangles and the dashed line of Fig. 2 shows such distribution. The vertical separation between the solid and the dashed line is 9.6 dB, which means that the expected number of echoes from the sidelobe region

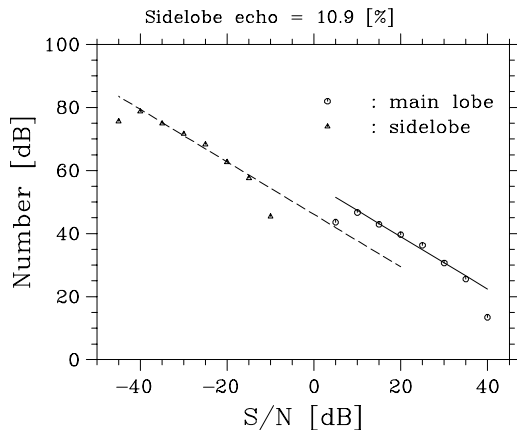


Fig. 2 Echo power distribution of detected meteors. Dashed line shows the estimated distribution of sidelobe contribution.

is 10.9% of those from the main lobe, assuring that majority of echoes are coming from the main lobe region.

If a target is in the main lobe region, at most three beams should show substantially larger echo power than the rest of the beam directions. This criterion is used to eliminate individual sidelobe echoes in the data processing.

#### 4. Determination of range and Doppler velocity

In order to detect weak meteor head echoes at a range of about 100 km, it is advantageous to use a long pulse of more than 100 μs, which has a narrow bandwidth of less than 10 kHz. The pulse width used in this observation is 256 μs, whose bandwidth is 4 kHz. On the contrary, the large Doppler shift of 22 kHz corresponding to the impinging velocity of 72 km/s does not allow the integration over the entire pulse width. We thus sample the received signal at a rate of 8 μs, take a series of 32 samples corresponding to the pulse width starting from each sample, and then take its Fourier transform of each series to obtain a Doppler power spectrum of the echo at that range sample. This process is equivalent to use 32 receivers of 4 kHz bandwidth with staggered center frequency at 4 kHz interval, and thus is called Doppler pulse compression hereafter. Fig. 3 schematically shows the principle and data flow of this procedure.

Fig. 4 shows an example of the meteor echo thus processed versus the Doppler velocity and the range. As is shown in the figure, a sharp peak is found at a frequency bin which matches to the velocity of the meteor. The meteor trail echoes which have a much lower Doppler velocity of less than about 100 m/s can be eliminated by removing the three center points of the spectrum.

The precise velocity is determined by interpolating between the three adjacent bins around the peak. Since the frequency response of each filter bank is known, the relative Doppler velocity Δv of the echo from that of the maximum point is computed from the ratio of the power of the maximum point to the secondary point, which is given by

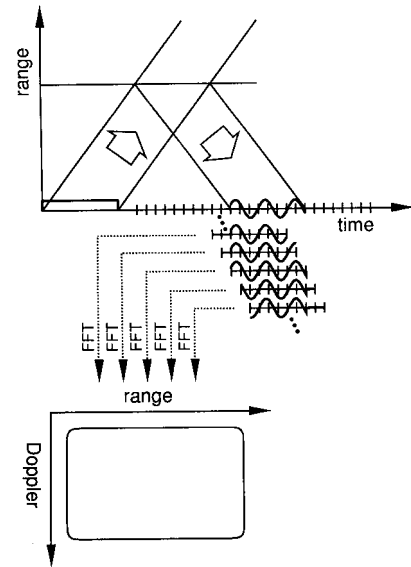


Fig. 3 Principle of Doppler pulse compression.

18-NOV-1998 04:38:23.10  
 Az0=116.0, Ze0= 24.0  
 Rec.= 7:001, Beam= 3  
 P<sub>max</sub>=100.3dB (V= 65.8km/s, R=111.5km)

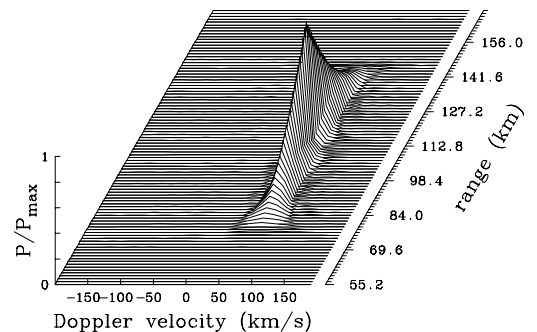


Fig. 4 Example of a meteor echo after Doppler pulse compression. Echo power is plotted versus height and Doppler velocity.

$$R(\Delta v) = \frac{S(\Delta v)}{S(v_o - \Delta v)} \tag{1}$$

where

$$S(v) = \left\{ \frac{\sin(\pi v/v_o)}{\pi v/v_o} \right\}^2 \tag{2}$$

and  $v_o(=12.6 \text{ km/s})$  is the spacing between the Doppler velocity bins. We made a lookup table of this function to determine Δv from the observed value of R.

Along the range direction, a triangular response, which is the auto-correlation function of the rectangular pulse, can be seen. The echo power and the range of the meteor is determined from the height and the location of the peak of this triangular shape by fitting the theoretical shape of the

**Table 1** Observation period during Leonid meteor storm.

Date: November 18, 1998			
Local time (JST)	Azimuth (deg)	Zenith (deg)	Obs. period (JST)
3:45	101	36	3:37-3:52
4:45	116	24	4:37-4:52
5:45	150	15	5:37-5:52
6:45	206	15	6:37-6:52
7:45	241	23	7:37-7:52
8:45	258	35	8:37-8:52

auto-correlation function. Right panels of Fig. 1 show the variation of echo power (top right), Doppler velocity (middle right), and height (bottom right) versus time after detection. The rapid variation of the echo power is due to different beam directions for successive pulses. Its upper envelope corresponds to the value observed by the center beam, which is sampled twice by beam No. 1 and 5 in each beam cycle. The decrease of the Doppler velocity indicates the deceleration due to atmospheric drag.

## 5. Preliminary results

The observation was made during the expected maximum of Leonid meteor storm on November 18, 1998 in JST. Six 15-minute periods shown in Table 1 were used for the present observation mode, and the radar was set to detect meteor trails for the rest of the time. During each period, the center of the beam groups was pointed to the expected radiant of Leonid stream meteors as shown in the table.

About 4,000 head echoes from the meteors were observed with sufficient intensity during this period. In order to determine the direction by using the method as described above, however, it is necessary to detect the same meteor over at least three consecutive pulses. About 530 cases satisfied this condition, for which the location can be determined for at least one pulse cycle consisting of 8 pulses. If the instantaneous position can be determined for two or more pulse cycles, the velocity vector can be determined. We have so far successfully determined the orbit for 235 events, although the analysis program is still under way of improvement. The points plotted in the left panel of Fig. 1 are the example of such determination. Three right panels in the figure shows the variation of echo power, Doppler velocity, and the height, respectively. This example is one of the strongest meteors, and was observed over 7 pulse cycles. The decay of Doppler velocity in time indicates the deceleration due to atmospheric drag.

Fig. 5 show the distribution of the direction of the velocity vector plotted versus the azimuth and zenith angle relative to the radiant of the Leonids. Different symbols indicate number of beam cycles during which each echo is observed. As is clearly shown in the figure, the observed meteors shows a large spreading whose standard deviation is about  $18^\circ$  in their direction. Part of the scatter is due to the error in determining the instantaneous location of the meteor caused by the fluctuations of the echo power during the three adjacent pulse period. It is confirmed from the fact that the standard

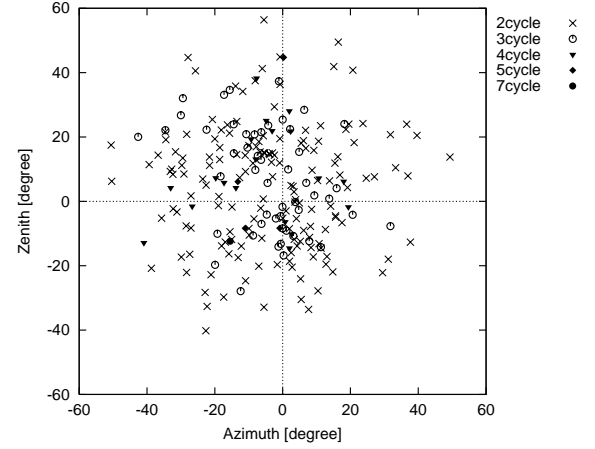


**Fig. 5** Directional distribution of velocity vector of the meteors around the expected radiant. Different symbols indicate number of beam cycles during which each echo is observed.

deviation monotonically decreases when the data is classified according to the number of beam cycles.

The magnitude of this error is estimated by comparing the standard deviation of this standard deviation for different number of beam cycles. We first assume that the cross-range distance of each data point used in determining the velocity vector has a Gaussian random error with standard deviation  $\sigma_e$  independent of the duration of each meteor. For the case when an echo is observed for two or more pulse cycles, the direction of the velocity vector is simply given by the direction of the straight line connecting the two points. Thus the angular error due to  $\sigma_e$  is given by

$$\epsilon_2 = \tan^{-1}(\sqrt{2}\sigma_e/\Delta r) \cong \sqrt{2}\sigma_e/\Delta r \quad (3)$$

where  $\Delta r$  is the range difference between the two points. The subscript 2 denotes the number of pulse cycles. For the case when an echo is observed for  $N(> 2)$  pulse cycles, the direction is determined by fitting a straight line to these data points. The angular error is given by

$$\epsilon_N \cong \sigma_e / \sqrt{\sum_{i=1}^N r_i^2} \quad (4)$$

where  $r_i$  is the range at each pulse cycle, and we take the coordinate that  $\sum r_i = 0$ . Assuming that  $r_i$  is uniformly distributed, which is valid as a first order approximation, we get

$$\begin{aligned} \epsilon_3 &= \epsilon_2/2 \\ \epsilon_4 &= \epsilon_2/\sqrt{10} \\ \epsilon_5 &= \epsilon_2/\sqrt{20} \end{aligned}$$

and so on. The observed standard deviation for the  $N$ -cycle case is given by

$$\sigma_N = \sqrt{\sigma^2 + \epsilon_N^2}, \quad (5)$$

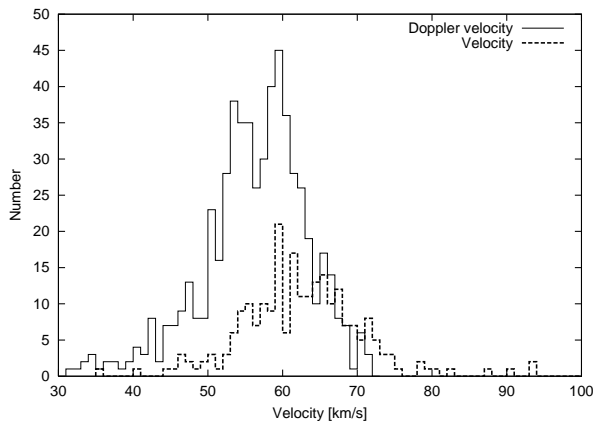


Fig. 6 Doppler velocity (solid line) and absolute velocity (dashed line) distribution of detected meteors.

where  $\sigma$  is the true scatter of the velocity vector. We can thus estimate both  $\sigma$  and  $\epsilon_2$  from the data shown in Fig. 5 to be  $13.4^\circ$  and  $14.3^\circ$ , respectively. This result also indicates that the data points observed for 4 or more beam cycles are free from the observational error.

The large value of more than  $10^\circ$  of the true (or natural) scatter of the directions seems to be too large compared to that of bright Leonid stream meteors, whose standard deviation derived from optical observation is about  $0.5^\circ$ [1]. It suggests that the very weak meteors detected by the MU radar are dominated by sporadic meteors rather than the stream meteors associated with the Leonids storm. It gives an important information on the brightness distribution of the Leonid meteors.

Fig. 6 shows the distribution of the Doppler velocity and the magnitude of the velocity vector. A sharp cut off at around 72 km/s seen in Doppler velocity in Fig. 6 confirms the validity of velocity determination because it is the expected maximum velocity of an orbiting object relative to the earth in the solar system. The reason that the distribution has its peak in a very fast range of 50–60 km/s region is probably due to the fact that the current observation is made around the dawn when the apex of the earth is close to the zenith. During such a period, even sporadic meteors tend to have a large impinging velocity biased to the velocity of the earth itself. Velocity of less than 25 km/s cannot be measured by the current observational setup, which eliminates the low velocity component to remove meteor trail echoes. The total velocity shown in Fig. 6 shows that the peak is actually in a even higher region of 60–65 km/s. Smaller numbers are due to the fact that correspond to limited cases where the echo was observed for two or more beam cycles. Several points above the maximum velocity may indicate the errors in determining the direction, or the existence of very fast interstellar meteors.

## 6. Summary

We developed an observation scheme to detect weak head echoes of very fast meteors associated with Leonid meteor storm, and to determine their orbit. The direction was successfully determined by making use of the fast beam steerability of the MU radar, and the range and velocity was estimated using the Doppler pulse compression. This experiment enabled to determine the distribution of both the direction and magnitude of the velocity vector of the meteor head echoes for the first time. A preliminary analysis of the data during the Leonid meteor storm suggests that very weak meteor echoes are dominated by sporadic meteors even near the peak of the storm.

In order to reduce the error in determining the direction, a mono-pulse capability was added to the observation scheme by separately recording the received signals from three subsets of the antenna array. It was applied to the observation on November 18, 1999, although the analysis of the data has just been started.

## Acknowledgment

The authors thank Mr. R. Shimizu, who is currently with the Institute of Space and Astronomical Science, for his help in data analysis and software development while he was with School of Electrical and Electronic Engineering, Kyoto University. The MU radar belongs to, and is operated by Radio Atmospheric Science Center, Kyoto University. This study is carried out as a part of "Ground Research Announcement for Space Utilization" promoted by Japan Space Forum.

## References

- [1] Betlem, H., Jenniskens, P., Leven, J., Kuile, C., Johannink, C., Zhao, H., Lei, C., Li, G., Zhu, J., Evans, S., and Spurny, P., "Very precise orbits of 1998 Leonid meteors," *Meteorit. Planet. Sci.*, vol. 34, no. 6, pp. 979–986, Nov. 1999.
- [2] Kessler, D. J., "Orbital debris environment for spacecraft in low earth orbit," *Journal of Spacecraft and Rockets*, vol. 28, no. 3, pp. 347–351, May 1991.
- [3] Fukao, S., Sato, T., Tsuda, T., Kato, S., Wakasugi, K., and Makihiro, T., "The MU radar with an active phased array system, 1. Antenna and power amplifier," *Radio Sci.*, vol. 20, no. 6, pp. 1155–1168, Nov. 1985.
- [4] Sato, T., Kayama, H., Furusawa, A., and Kimura, I., "MU radar measurements of orbital debris," *J. Spacecraft and Rockets*, vol. 28, no. 6, pp. 677–682, Nov. 1991.
- [5] Nakamura, T., Tsuda, T., Tsutsumi, M., Kita, K., Uehara, T., Kato, S., and Fukao, S., "Meteor wind observations with the MU radar," *Radio Sci.*, vol. 26, no. 4, pp. 857–869, July 1991.
- [6] Wannberg, A. P., and G. Wannberg, "Meteor observations with the European incoherent scatter UHF radar," *J. Geophys. Res.*, vol. 99, no. A6, pp. 11379–11390, June 1994.
- [7] Verniani, F., "An analysis of the physical parameters of 5759 faint radio meteors," *J. Geophys. Res.*, vol. 78, no. 35, pp. 8429–8462, Dec. 1973.
- [8] Sato, T., Wakayama, T., Tanaka, T., Ikeda, K., and Kimura, I., "Shape of space debris as estimated from RCS variations," *J. Spacecraft and Rockets*, vol. 31, no. 4, pp. 665–670, July 1994.
- [9] Fukao, S., Sato, T., Tsuda, T., Yamamoto, M., Yamataka, M. D., and Kato, S., "MU radar: New capabilities and system calibrations," *Radio*

*Sci.*, vol. 25, no. 4, pp. 477–485, July 1990.

**Toru Sato** received his B.E, M.E., and Ph.D. degrees in electrical engineering from Kyoto University, Kyoto, Japan in 1976, 1978, and 1982, respectively. He has been at Kyoto University since 1983 and is currently a Professor of Department of Communications and Computer Engineering, Graduate School of Informatics. His major research interests have been system design and signal processing of atmospheric radars, radar remote sensing of the atmosphere, observations of precipitation using radar and satellite signals, radar observation of space debris, and signal processing for subsurface radars. He was awarded Tanakadate Prize in 1986. He is a member of the Institute of Electrical and Electronics Engineers, the Japan Society for Aeronautical and Space Sciences, the Society of Geomagnetism and Earth, Planetary and Space Sciences, and American Meteorological Society.

**Takuji Nakamura** received his B.E., M.E., and Ph.D. degrees in electrical engineering from Kyoto University, Kyoto, Japan in 1984, 1986, and 1992, respectively. Since 1986, he worked for Mitsubishi Electric Co. and since 1989 he has been with Radio Atmospheric Science Center, Kyoto University. In April 2000, the name of the center was changed as Radio Science Center for Space and Atmosphere. Currently, he is an associate professor in the center. His major research interests have been system design and signal processing of atmospheric radars, radar and optical remote sensing techniques of the atmosphere, dynamics and aeronomy of the earth's middle atmosphere, and radio scattering mechanism of meteor phenomena. He was awarded Obayashi Prize of the Society of Geomagnetism and Earth, Planetary and Space Sciences in 1997. He is a member of the Society of Geomagnetism and Earth, Planetary and Space Sciences, the Meteorological Society of Japan, the Astronomical Society of Japan and the American Geophysical Union.

**Koji Nishimura** received his B.E. in electrical engineering from Ritsumeikan University, Kyoto, Japan in 1999, and entered Department of Communication and Computer Engineering, Graduate School of Informatics, Kyoto University. He is currently working for his Master's degree. His research interest has been radar signal processing.